Supporting Information for

Tailoring the Subshell and Electronic Structure of Atomically Precise AuAg Alloy Nanocluster

Guocheng Deng,[a,b,⊥] Taeyoung Ki,[a,b,⊥] Xiaolin Liu,[a,b,⊥] Yuping Chen,[c,⊥] Kangjae Lee,[a,b] Seungwoo Yoo,[a,b] Qing Tang,[c,*] Megalamane S. Bootharaju,[a,b,*] and Taeghwan Hyeon[a,b,*]

[a]*Center for Nanoparticle Research, Institute for Basic Science (IBS), Seoul 08826, Republic of Korea.*

[b]*School of Chemical and Biological Engineering, and Institute of Chemical Processes, Seoul National University, Seoul 08826, Republic of Korea.*

[c]*School of Chemistry and Chemical Engineering, Chongqing Key Laboratory of Theoretical and Computational Chemistry, Chongqing University, Chongqing 401331, China.*

*Email: qingtang@cqu.edu.cn, msbootharaju@snu.ac.kr, thyeon@snu.ac.kr

[⊥]G.D., T.K., X.L., and Y.C. contributed equally to this work.

EXPERIMENTAL SECTION

Reagents. Hydrogen tetrachloroaurate(III) trihydrate ($HAuCl_4 \cdot 3H_2O$) was purchased from Strem. Triethylamine (Et_3N), silver nitrate ($AgNO_3$), silver acetate (CH_3COOAg), sodium methoxide (CH_3ONa), trans-2-[3-(4-tert-butylphenyl)-2-methyl-2-propenylidene]malononitrile (DCTB), and tetraphenylphosphonium tetraphenylborate (PPh_4BPh_4) were purchased from Sigma-Aldrich. 3,4-difluorophenylacetylene (HC≡CR), phenylacetylene (HC≡CPh), dimethyl sulfide ($(CH_3)_2S$) and borane *tert*-butylamine complex ($BH_3 \cdot C_4H_{11}N$) were purchased from TCI. Dichloromethane (CH_2Cl_2), methanol (CH_4O), acetonitrile (CH_3CN), acetone (CH_3COCH_3) and *n*-hexane (C_6H_{14}) were purchased from Samchun. $AuSMe_2Cl$[1] and $Au_{34}Ag_{28}(C{\equiv}CPh)_{34}$[2] were prepared according to literature method. The water used in all experiments was ultrapure. All reagents were used as received without further purification.

Synthesis of AgC≡CR: 340 mg of $AgNO_3$ was dissolved in 20 mL of acetonitrile, followed by the subsequent addition of 242 μL of 3,4-difluorophenylacetylene. Then, 400 μL of triethylamine was added to the solution with vigorous stirring. The reaction mixture was left to stir for 4 hours at room temperature in the absence of light. Afterward, the obtained turbid mixture was centrifuged at 8000 rpm for 1 min. The precipitate was washed with 30 mL of methanol and then dried in vacuum at room temperature to give a gray AgC≡CR complex. The yield of the complex was ~81% (based on Ag).

Synthesis of AuC≡CR: 591 mg of $AuSMe_2Cl$ was dispersed in 30 mL of acetone, to which 242 μL of 3,4-difluorophenylacetylene was added subsequently. Then, 300 μL of triethylamine was added to the above solution under vigorous stirring. The reaction mixture was stirred for 1 hour at room temperature in absence of light. The solution was then subjected to evaporation until dryness, resulting in the formation of a yellow solid. This solid was subsequently washed with 30 mL of water and 15 mL of methanol. Then the yellow solid was dried in vacuum at room temperature to give a yellow AuC≡CR complex in a yield of ~83% (based on Au).

Synthesis of $Au_{34}Ag_{27}$ nanocluster: The synthesis of **$Au_{34}Ag_{27}$** was carried in a small vial at 25 °C in ambient air. Specifically, 6.7 mg of AuC≡CR and 4.9 mg of AgC≡CR were dispersed in a mixed solution of CH_2Cl_2 (3 mL) and CH_3OH (1 mL). Subsequently, 1 mg of PPh_4BPh_4 solid was added to the above solution while maintaining vigorous stirring (600 rpm). After stirring for 5 minutes, a solution of 3 mg of borane tert-butylamine complex in 1 mL of CH_2Cl_2 was added dropwise. This led to the dissolution of the suspension and a gradual change in the solution's color to red and then brown. The solution was left to age for 18 hours. The resulting solution was washed once with water by adding 5 mL of water and shaking for 1 minute. The aqueous phase was removed, and the organic phase was centrifuged at 12,000 rpm for 5 minutes. The precipitate was discarded, and the organic solution (2 mL) underwent vapor diffusion of *n*-hexane (15 mL) at 25 °C. After 7 days, black block crystals were obtained with a yield ranging from 4-6% (based on Au).

Physical measurements: The UV/vis absorption spectra were recorded using a Cary 5000 spectrophotometer (Agilent). The scanning electron microscopy energy dispersive X-ray spectroscopy (SEM-EDS) analysis was performed on a JSM-7800F Prime microscope (JEOL, Japan). Matrix-assisted laser desorption ionization-time of flight-mass spectrometry (MALDI-TOF-MS) of the nanoclusters was performed using AB SCIEX TOF/TOFTM5800 mass spectrometer (AB Sciex, MA, USA) installed at the Korea Basic Science Institute (KBSI), Seoul center.

Single crystal structure analysis. The diffraction data of $\mathbf{Au_{34}Ag_{27}}$ were collected by X-ray single crystal diffractometer with Cu Kα radiation (λ = 1.54184 Å) at 100 K on a Rigaku XtaLab Synergy R system. The data were processed using CrysAlis^{Pro}.[3] The structure was solved and refined using Full-matrix least-squares based on F^2 with program ShelXT and ShelXL within Olex2.[4-6] SQUEEZE tool of PLATON was applied, due to large solvent (*n*-hexane and DCM) voids in the structure. A solvent mask was calculated and 726 electrons were found in a volume of 2791 Å^3 in six voids per unit cell. This is consistent with the presence of ten CH_2Cl_2 and six C_6H_{14}, per asymmetric unit which account for 720 electrons per unit cell. More refined data are provided in Table S1.

Computational details. To simplify the calculation, all C ≡ C-R (HC ≡ CR is 3,4-difluorophenylacetylene) ligands are replaced with C ≡ C-CH_3 groups. As for optical-absorption spectrum and orbital information, the density functional theory (DFT) calculations were performed by employing the CP2K package.[7] The electronic structure calculations are described by DFT with the spin-polarized Perdew−Burke−Ernzerhof (PBE) functional and mixed double-ζ Gaussian and plane-wave (GPW) basis sets with an energy cutoff of 350 Ry.[8] Core electrons have been modeled by Goedecker−Teter−Hutter (GTH) pseudopotentials with 11, 11, 4 and 1 valence electrons for Au, Ag, C and H, respectively. The DFT-D3 method proposed by Grimme et al. was adopted to better describe the noncovalent interactions.[9,10] Then, the time-dependent DFT (TDDFT) computation of optical absorption spectrum was performed at the PBE level with the DZVP-MOLOPT-SR-GTH basis sets. Based on the above results, the Multiwfn program can be used to process and plot UV-Vis spectrum.[11]

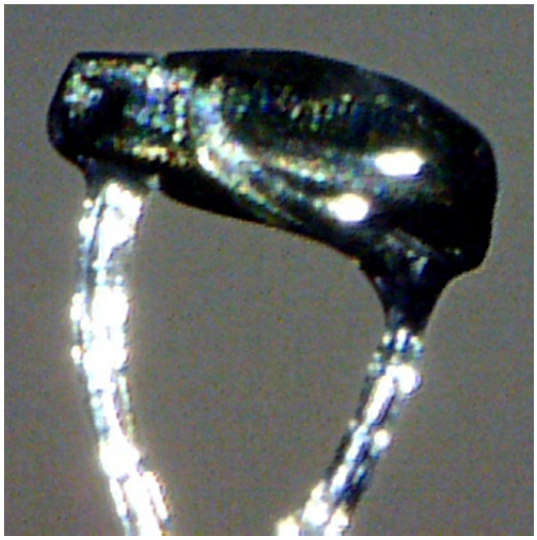

Figure S1. A photograph of the single crystal of the $\mathbf{Au_{34}Ag_{27}}$ nanocluster.

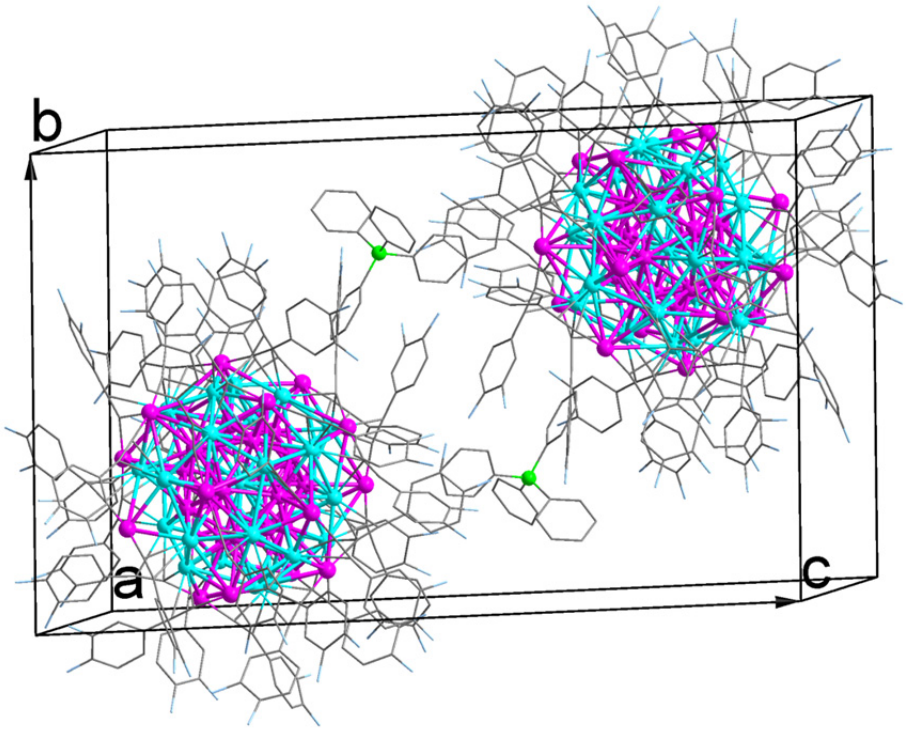

Figure S2. The packing diagram of $\mathbf{Au_{34}Ag_{27}}$. Color legend: magenta, Au; turquoise, Ag; green, P; pale blue, F; gray, C. All hydrogen atoms are omitted for clarity.

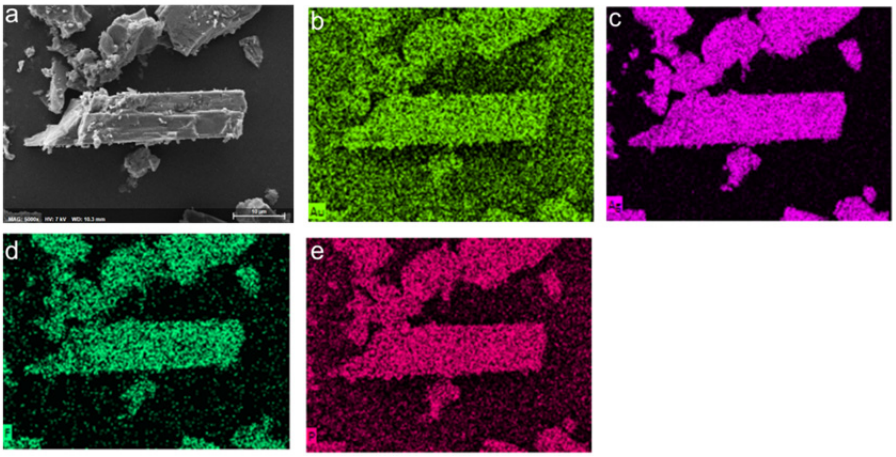

Figure S3. (a) SEM image of a crystal of $\mathbf{Au_{34}Ag_{27}}$. (b-e) EDS mapping images of Au, Ag, F and P, respectively, of the $\mathbf{Au_{34}Ag_{27}}$ crystals. The background signal in the elemental map b is originated from Pt, which was coated to avoid sample charging during SEM-EDS measurement.

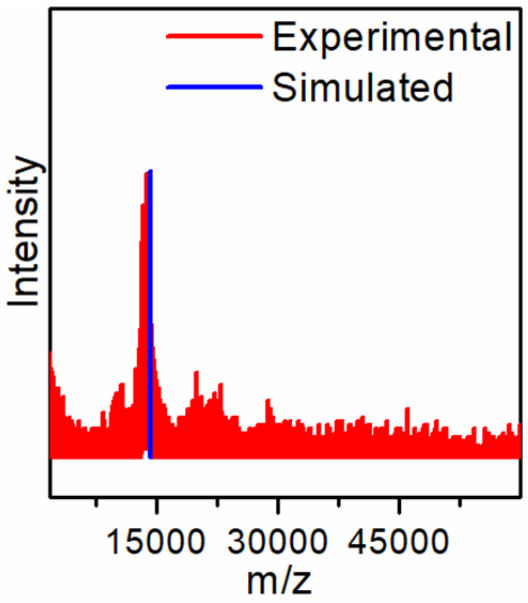

Figure S4. Experimental and Simulated mass spectra of $\mathbf{Au_{34}Ag_{27}}$.

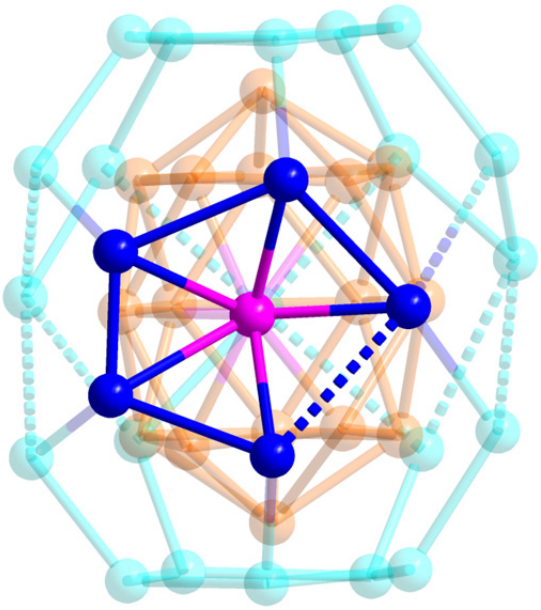

Figure S5. Each of the faces of the third shell of **$Au_{34}Ag_{27}$** covers a gold atom from the second shell. Color legend: orange and magenta, Au; turquoise and blue, Ag.

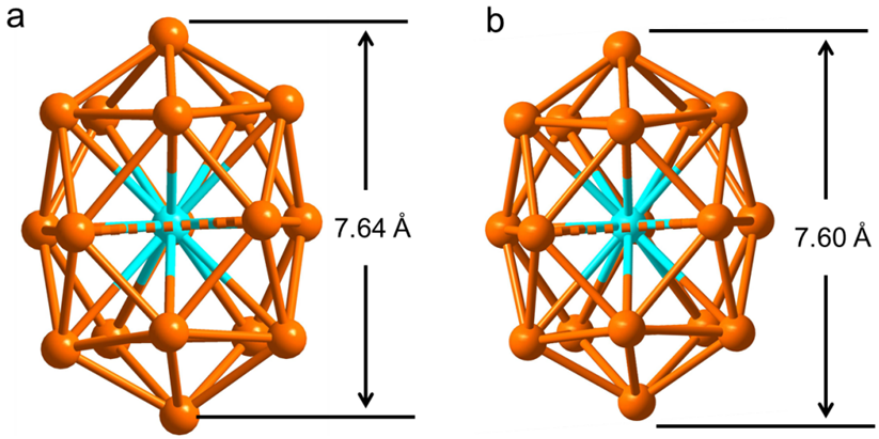

Figure S6. Structural comparison of the first and second shells ($Ag_1@Au_{17}$) of **$Au_{34}Ag_{27}$** (a) and **$Au_{34}Ag_{28}$** (b) nanoclusters. Color legend: orange, Au; turquoise, Ag.

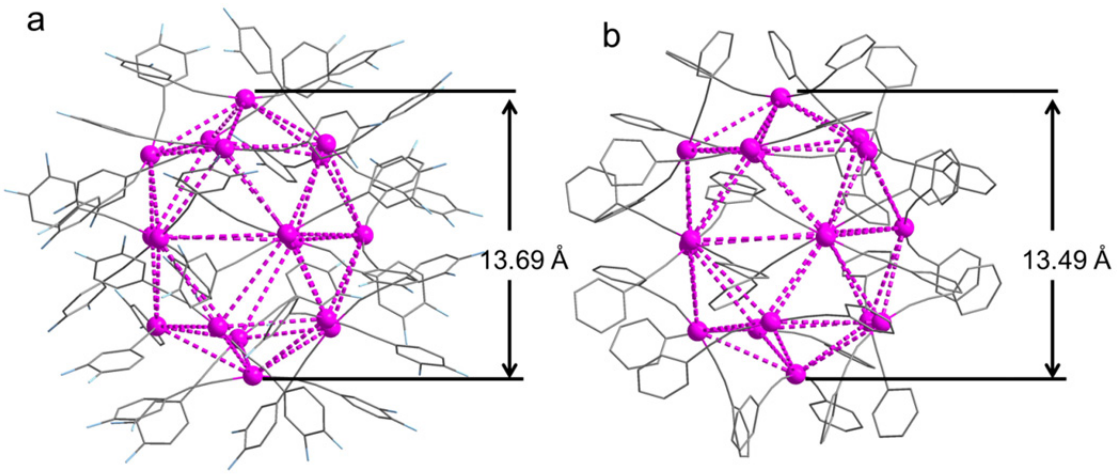

Figure S7. Structural comparison of the fourth shell (Au_{17}) of **$Au_{34}Ag_{27}$** (a) and **$Au_{34}Ag_{28}$** (b) nanoclusters.

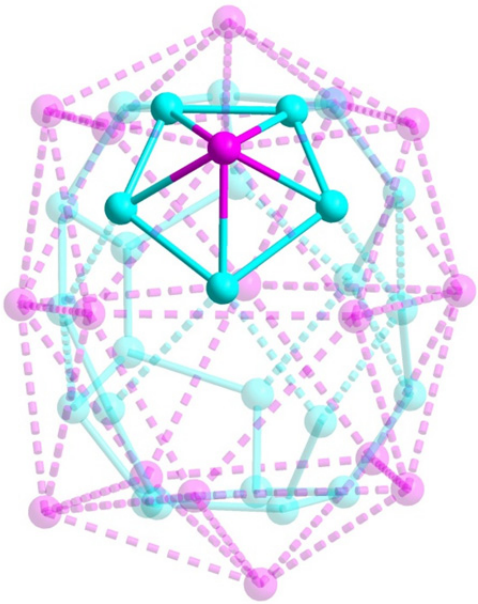

Figure S8. Each gold atom of the fourth shell of **$Au_{34}Ag_{27}$** caps one face of the third shell. Color legend: magenta, Au; turquoise, Ag.

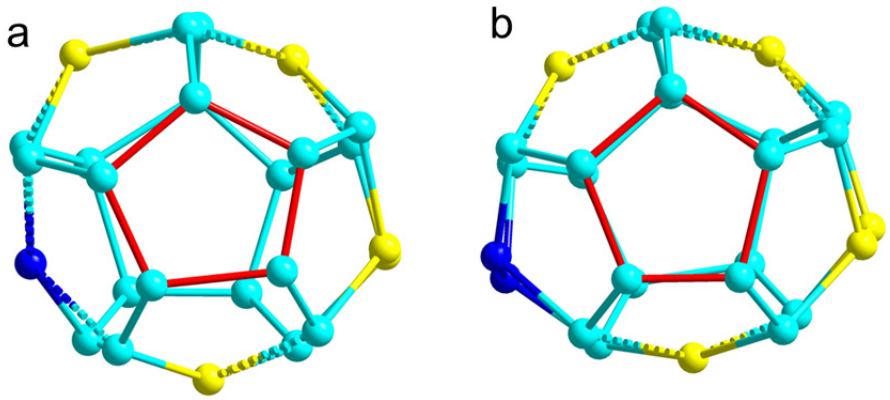

Figure S9. Top view of the third shell of the $\mathbf{Au_{34}Ag_{27}}$ (a) and $\mathbf{Au_{34}Ag_{28}}$ (b) nanoclusters. Color legend: turquoise, blue, and yellow, Ag.

Table S1. The crystal data and structure refinement for the **$Au_{34}Ag_{27}$** nanocluster.

Identification code	**$Au_{34}Ag_{27}$**
Empirical formula	$C_{296}H_{122}Ag_{27}Au_{34}F_{68}P$
Formula weight	14610.25
Temperature/K	100(2)
Crystal system	triclinic
Space group	*P*-1
a/Å	21.0215(2)
b/Å	22.1806(2)
c/Å	35.4832(3)
α/°	88.1010(2)
β/°	74.9280(3)
γ/°	87.3240(2)
Volume/Å^3	15945.4(3)
Z	2
ρ_{calc}g/cm^3	3.041
μ/mm^{-1}	42.251
F(000)	12960.0
Crystal size/mm^3	0.532 × 0.187 × 0.152
Radiation	Cu Kα (λ = 1.54184)
2Θ range for data collection/°	5.824 to 133.196
Index ranges	$-25 \leq h \leq 16$, $-26 \leq k \leq 26$, $-42 \leq l \leq 42$
Reflections collected	156980
Independent reflections	55473 [R_{int} = 0.1144, R_{sigma} = 0.1066]
Data/restraints/parameters	55473/2578/3151
Goodness-of-fit on F^2	1.120
Final R indexes [I>=2σ (I)]	R_1 = 0.1081, wR_2 = 0.2649
Final R indexes [all data]	R_1 = 0.1213, wR_2 = 0.2746
Largest diff. peak/hole / e Å^{-3}	7.73/-6.18

References

1) N. Nishina and Y. Yamamoto, *Synlett*. 2007, **11**, 1767-1770.
2) Y. Wang, X. Wan, L. Ren, H. Su, G. Li, S. Malola, S. Lin, Z. Tang, H. Häkkinen, B. K. Teo, Q. Wang and N. Zheng, *J. Am. Chem. Soc.* 2016, **138**, 3278-3281.
3) *CrysAlisPro*, version 1.171.135.119; Agilent Technologies Inc.: Santa Clara, CA, 2011.
4) O. V. Dolomanov, L. J. Bourhis, R. J. Gildea, J. A. K. Howard and H. Puschmann, *J. Appl. Crystallogr.* 2009, **42**, 339-341.
5) G. M. Sheldrick, *Acta Crystallogr. Sect. A: Found. Crystallogr.* 2008, **64**, 112-122.
6) G. M. Sheldrick, *Acta Crystallogr. Sect. A: Found. Adv.* 2015, **A71**, 3-8.
7) J. VandeVondele, M. Krack, F. Mohamed, M. Parrinello, T. Chassaing and J. Hutter, *Comput. Phys. Commun.* 2005*,* **167***,* 103−128.
8) J. P. Perdew, K. Burke and M. Ernzerhof, *Phys. Rev. Lett.* 1996, **77**, 3865−3868.
9) S. Grimme, J. Antony, S. Ehrlich and H. Krieg, *J. Chem. Phys.* 2010, **132**, 154104.
10) S. Grimme, S. Ehrlich and L. Goerigk, *J. Comput. Chem.* 2011, **32**, 1456−1465.
11) T. Lu and F. Chen, *J. Comput. Chem.* 2012, **33**, 580-592.